

## Article

# Evaluation of the Gas Emissions during the Thermochemical Conversion of Eucalyptus Woodchips

João Silva <sup>1,2,\*</sup> , Carlos Castro <sup>1</sup> , Senhorinha Teixeira <sup>2</sup>  and José Teixeira <sup>1</sup> <sup>1</sup> METRICs Research Centre, University of Minho, 4800-058 Guimarães, Portugal<sup>2</sup> ALGORITMI Research Centre/LASI, University of Minho, 4800-058 Guimarães, Portugal

\* Correspondence: js@dem.uminho.pt

**Abstract:** The combustion of solid biomass in industrial boilers involves a sequence of processes that include heating, drying, devolatilization, and char conversion. To maintain a repeatable and fully controlled environment, and to monitor all the dynamics involved in the phenomena at a real scale, field-scale experiments become necessary to perform investigations. In this way, to evaluate different thermochemical conversion conditions of biomass particles under an oxidative atmosphere, and to quantify the emission of the main gas compounds continuously, a small-scale reactor was developed and presented in this paper. Hence, in this work, larger particles of eucalyptus are burned at 400 and 800 °C under different stoichiometric conditions to understand the differences between different biomass conversion regimes (gasification and combustion). The analysis of the mass loss at the different temperatures was characterized by only two different and consecutive stages for both thermochemical conditions. The first region does not present the influence on the air flow rate; however, there is a significant difference in the second region. This fact highlighted the importance of the diffusion of oxygen during the char conversion. Regarding the quantification of the gas compounds, an increase of around 3 times in the CO and CO<sub>2</sub> emissions when gasification occurs was observed at 400 °C. However, at 800 °C, the same trend was verified, also verifying a considerable amount of CH<sub>4</sub>.

**Keywords:** biomass; combustion; gas emissions; macro thermogravimetric analysis; pyrolysis; woodchips



**Citation:** Silva, J.; Castro, C.; Teixeira, S.; Teixeira, J. Evaluation of the Gas Emissions during the Thermochemical Conversion of Eucalyptus Woodchips. *Processes* **2022**, *10*, 2413. <https://doi.org/10.3390/pr10112413>

Academic Editors: Ali Umut Sen, Catarina Pereira Nobre and Terencio Rebello de Aguiar Junior

Received: 30 September 2022

Accepted: 12 November 2022

Published: 16 November 2022

**Publisher's Note:** MDPI stays neutral with regard to jurisdictional claims in published maps and institutional affiliations.



**Copyright:** © 2022 by the authors. Licensee MDPI, Basel, Switzerland. This article is an open access article distributed under the terms and conditions of the Creative Commons Attribution (CC BY) license (<https://creativecommons.org/licenses/by/4.0/>).

## 1. Introduction

Solid biomass fuels, unlike fossil fuels such as coal, do not take millions of years to develop and, every year, a vast amount of biomass grows through the photosynthesis process by absorbing CO<sub>2</sub> from the atmosphere. Solid biomass is thus considered a renewable energy source and an interesting route to diversify energy production and reduce the dependence on fossil fuels [1]. Eucalyptus is the most representative solid biomass species in Portugal [2]. It was reported in 2015 that this species occupied 882,000 ha of the total forest area. It is still growing and is a major resource for paper production as well as fuel for heat production (both in households and in industry) [3]. Although the major source of solid biomass comes from the trunk, the literature emphasizes other streams of solid biomass with high potential. As an example, Roman et al. [4] have studied the potential of forest waste biomass for briquette production. Such works are a major contribution to the area as they present alternatives for the current solid biomass streams.

Regarding the main technological pathways for the production of heat and power, or combined heat and power, through the utilization of solid biomass, combustion and gasification are the main options [5]. Combustion represents one of the oldest technologies of biomass thermochemical conversion and utilization. The combustion process is an exothermic reaction between oxygen and biomass-volatile compounds that produce heat. The heat released is the main source of energy used in this process [6]. In a typical biomass combustion process, three main stages can be observed: drying, devolatilization, and char

burning. The drying stage is associated with the water evaporation present in the biomass. During the devolatilization stage, volatile compounds are released and burned with the oxygen present in the atmosphere. For the char combustion stage, the remaining carbon reacts with the oxygen, leaving ashes at the end of the combustion [7,8]. In the operation of biomass boilers, the design of the air supply system, including primary and secondary air, plays an important role in the combustion efficiency of biomass [9,10]. Yin et al. [11] reported that for grate-firing, one of the main technologies in biomass combustion, the overall excess air is usually set to 25% or above.

In its turn, gasification consists of burning biomass with insufficient oxygen under sub-stoichiometric conditions to produce combustible gases, which are collectively referred to as syngas. This is an attractive method of efficient energy extraction, mainly because a considerable amount of CO and CH<sub>4</sub> are obtained in comparison with combustion. Hence, in solid biomass gasification, an air-to-fuel ratio around 1.5:1 to 1.8:1 is necessary, while a combustion ratio is around 3.8:1 [12].

Since, in both technologies, the main stages of biomass thermochemical conversion remain the same, the study and comprehension of the gas-release evolution in a practical way can provide knowledge to develop computer models or to design equipment, such as furnaces, stoves, boilers, and gasifiers [13]. Among the three stages, devolatilization is considered one of the most important for heat and power generation. Hence, it is related to the oxidation, under different stoichiometric conditions depending on the conversion technology, of the volatile compounds and has a significant impact on the exothermic reaction. For that reason, it is also important to study and understand the composition of the gas released during the devolatilization stage. Usually, complete combustion yields only CO<sub>2</sub> and H<sub>2</sub>O as reaction products. However, other compounds can be formed, such as CH<sub>4</sub>, CO, and H<sub>2</sub>, increasing pollutant emissions and contaminating the environment [14].

To study the thermochemical conversion behavior of solid biomass, TGA (Thermo Gravimetric Analysis), a well-known thermal analysis technique and one of the most used, is applied [15,16]. Several authors have applied TGA to characterize the conversion of samples with a reduced size and mass in a kinetic way. However, TGA experiments are limited to assess the gas phase, and the lack of information in the literature relative to the gas emissions in this type of work persists [17–20]. Nevertheless, the gaseous release process analysis can be evaluated using the same technique but on a larger scale, commonly known as macro TGA [21]. In this way, the experiments are closer to the real thermochemical conversion processes, either in industrial or domestic equipment. Hence, macro TGA experiments take into account heat and mass transfer effects.

Regarding the literature concerning macro TGA experiments, Becidan et al. [22] presented the application of chromatography and spectrophotometry to study the gases released during the combustion of biomass residues. A fraction of the exhaust gases is collected and analyzed by a Fourier-Transform Infrared Spectroscopy (FTIR) analyzer and a micro-gas chromatograph. The FTIR was used to quantify CO<sub>2</sub>, CO, CH<sub>4</sub>, C<sub>2</sub>H<sub>2</sub>, and C<sub>2</sub>H<sub>4</sub>. The gas samples were also quantified online using a micro-gas chromatograph equipped with two thermal conductivity detectors and a double injector connected to two columns to separate and quantify CO<sub>2</sub>, hydrocarbons (CH<sub>4</sub>, C<sub>2</sub>H<sub>2</sub>, C<sub>2</sub>H<sub>4</sub>, and C<sub>2</sub>H<sub>6</sub>), and the remaining gases (H<sub>2</sub>, O<sub>2</sub>, CH<sub>4</sub>, CO, and N<sub>2</sub>) in another column. Brunner et al. [23] and Gauthier et al. [24] also applied both techniques to analyze the NO<sub>x</sub> emissions, ash release, and the main gaseous species and tar, respectively. Additionally, Weissinger et al. [25] described the release of nitrogen compounds using FTIR spectroscopy. Both works refer to the importance of the determination of nitrogen gaseous compounds that may serve as input profiles for Computational Fluid Dynamics (CFD) simulations. Bennadji et al. [26] and Nikku et al. [27] measured the fractions of light species from pyrolysis at low temperatures and compared the reactivity of municipal solid wastes with biomass and coal samples through the FTIR technique, respectively. Hu et al. [28] analyzed the influence of different atmospheres in the gaseous conversion using the mass spectrometer.

Although the quantification of the gaseous compounds released during the thermal conversion of biomass is not addressed, there are works in the literature where the conversion of biomass was analyzed separately through the macro TGA technique. Baumgarten et al. [29] and Samuelson et al. [30] analyzed the combustion behavior under typical isothermal conditions in the start-up of furnaces. Orang et al. [31] observed the effect of moisture content on combustion behavior. The author highlighted the higher drying and the ignition times due to the increase of the moisture content.

Thus, macro TGA experiments provide the possibility to control and maintain external heat fluxes in order to better represent, at a small-scale, the conditions expected in industrial boilers.

Gauthier et al. [24] used a purpose-built horizontal lamp tube reactor to perform pyrolysis of centimeter-scale wood particles, for temperatures ranging between 450 and 1050 °C. Yang et al. [32] studied the effect of the particle size (pinewood cubes ranging from 5 to 35 mm) on pinewood combustion in a batch reactor by measuring the mass loss rate and the temperature profile at different bed locations and gas composition in the out-of-bed flue gases. Ryu et al. [33] studied the combustion of four biomass materials with different fuel properties under fuel-rich conditions, measuring temperature, mass loss, and gas composition. Mahmoudi et al. [34] focused on developing a numerical model using the Euler-Lagrange model in which the fluid phase is a continuous phase and each particle is tracked with the Lagrangian approach to understand the combustion phase. This work was performed along with an experimental study, with temperature and mass loss monitoring, to validate the numerical model. Wurzenberger et al. [35] created a combined transient single particle and fuel-bed model of a furnace in order to optimize its efficiency and emissions by acquiring information about all the physical and chemical effects on the process. Markovic et al. [36] studied the combustion of wood waste with pre-heated primary air up to 350 °C and the secondary air distributed via nozzles above the waste layer. The authors measured temperature, gas composition, mass loss, and the influence of primary air speed, fuel moisture, and inert content on the combustion characteristics. Eric et al. [37] focused the study on the kinetics of loose biomass in a vertical tube reactor measuring the fuel mass loss rate, with two biomass combustion models (piston and batch model). Most of the testing conditions resemble the traditional (micro) TGA operation where the sample follows a pre-defined heating curve. Usually, this leads to heating rates well below those expected inside a furnace. Long et al. [38] reported an alternative approach in which the sample was introduced into a reactor set at a predefined temperature. The authors only reported mass loss rates. Lelis et al. [39] measured the mass loss and variation of the elemental composition of pine wood pellets. The authors used a macro TGA to investigate the influence of temperature and time on devolatilization of C, H, and N. The experiments were carried out at a constant temperature, and it was found that the rate of release of N is higher than other compounds. However, no information on the actual species formed was provided.

This work presents an experimental facility developed to study how biomass fuels may behave in industrial power plants. Thus, the mass loss profiles at different thermo-chemical conditions of eucalyptus woodchips are presented together with the composition of the gases released over time. Furthermore, it is important to point out that the motivation for this work is related to the need to understand the composition of the gas compounds released during the conversion of solid biomass particles. It is necessary to know the composition, the amount of pyrolysis products in different reactor thermal conditions, and the reaction rate of the particles. A recent investigation mentioned that numerical prediction inside a grate-fired boiler depends on the devolatilization kinetics mechanism, which can significantly affect the outputs from the bed model [40]. Most of the CFD models usually employed biomass elemental composition and enthalpy conservation equations or models, like that proposed by Thunman et al. [41] and Neves et al. [42], to determine the composition of pyrolysis products (e.g., [43]). However, the results of this type of approach can produce unrealistic results. Therefore, there is a clear need to develop macro TGA

experiments to obtain experimental information that may be used to develop mathematical models to describe the devolatilization of biomass. These models can be used as an input to CFD models for grate-type combustors.

## 2. Materials and Methods

### 2.1. Samples

The woodchips necessary for the macro TGA experiments were prepared from large eucalyptus trunks by means of a knife chipper. Hence, larger particles were obtained, with dimensions similar to the ones used in biomass power plants, ranging from a few millimeters up to hundreds of millimeters. The particles were then spread in a room to be air-dried and to reduce the moisture content. After this, the particles were then sieved, and the particle size distribution was assessed by horizontal screening according to the standard EN 15149-1:2010 Part 2 using sieves with square hole apertures of 3.15, 8, 16, and 50 mm. The most representative particle class size was between 8 to 16 mm, which is in agreement with the analysis carried out on a biomass power plant [44]. In this way, the particles within this class size were collected and used for the experimental program. At that time, and after being air-dried for approximately one month, the moisture content of the particles was observed to be between 10 to 15% (dry basis). The elemental and proximate composition of the particles was also evaluated considering the standards for solid fuel characterization (CEN/TS 15414:2006 and CEN/TS 15104:2005, respectively), and the results are presented in Table 1.

**Table 1.** Composition of the eucalyptus woodchips.

Proximate Analysis (wt.%, Dry Basis)		Ultimate Analysis (wt.%, Dry Ash Free)	
Volatile matter	88.90	Carbon	48.68
Ash	1.00	Hydrogen	6.91
Fixed carbon	10.10	Nitrogen	0.23
		Oxygen	44.18

### 2.2. Experimental Apparatus and Procedure

A lab-scale reactor to represent the different thermochemical conversion conditions of solid biomass particles was designed. During the design stage, some important constraints were addressed. The first issue was related to the possible amount of biomass in each experiment and the ease of access to the interior of the reactor in order to introduce the sample. This was particularly important in order to consider secondary reactions in the fuel bed appropriately and also to consider high heating rates of the fuel comparable to real-scale grate-fired boilers. Secondly, high flexibility regarding analytical equipment connected with the reactor, and easy handling during the experiment without any interference with the sample, was also important. Moreover, online recording of relevant operation data was paramount.

Hence, the reactor can replicate the behavior of a fuel sample used in different combustion or gasification devices and, thereby, evolve through the different reaction stages (drying, devolatilization, and char combustion). The reactor had a cylindrical shape, 200 mm in diameter and 350 mm in height. In the surrounding walls, there was a 2 kW electrical heater and refractory material to avoid heat losses. At the upper part of the reactor, there was a rotating lid with a rip of 10 mm to allow the connection of a small basket with the biomass particles to a digital scale. Furthermore, two type K thermocouples were connected to a digital temperature controller, Eurotherm brand, that controlled its operation. The desired temperature in the equipment can be defined in the set-point temperature, but there is no possibility to monitor and acquire their variation over time. There are other external devices necessary to develop the experiment. An external flowmeter and scale were used to control the gas flow rate supplied to the reactor and to measure the mass loss variation of the sample, respectively.

The weight measurement of the sample was carried out by using a perforated cylindrical basket of 60 mm in diameter and 50 mm in height inside the reactor, suspended from the digital scale by a stainless-steel wire of 2 mm in diameter. Consequently, as there were three different devices, a data acquisition and monitoring program was developed using LabVIEW software to centralize the information of the different parameters and to be able to record the data throughout the experiments. Consequently, the LabVIEW program continuously recorded the weight, air flow rate, and temperature. In addition to these devices, a portable gas analyzer, Rapidox 5100 model, was used to measure the main gas compounds (CO<sub>2</sub>, CO, H<sub>2</sub>, and CH<sub>4</sub>) released during the experiment. All the gases have a  $\pm 1\%$  full scale accuracy and a 0.1% resolution. The collection and analysis of the gas samples were only possible through the utilization of a vacuum pump and a particle and moisture filter.

Thus, the mass loss and the gas emissions during each experiment are measured over time. Figure 1 presents a schematic diagram of the apparatus involved in the macro TGA experiments.

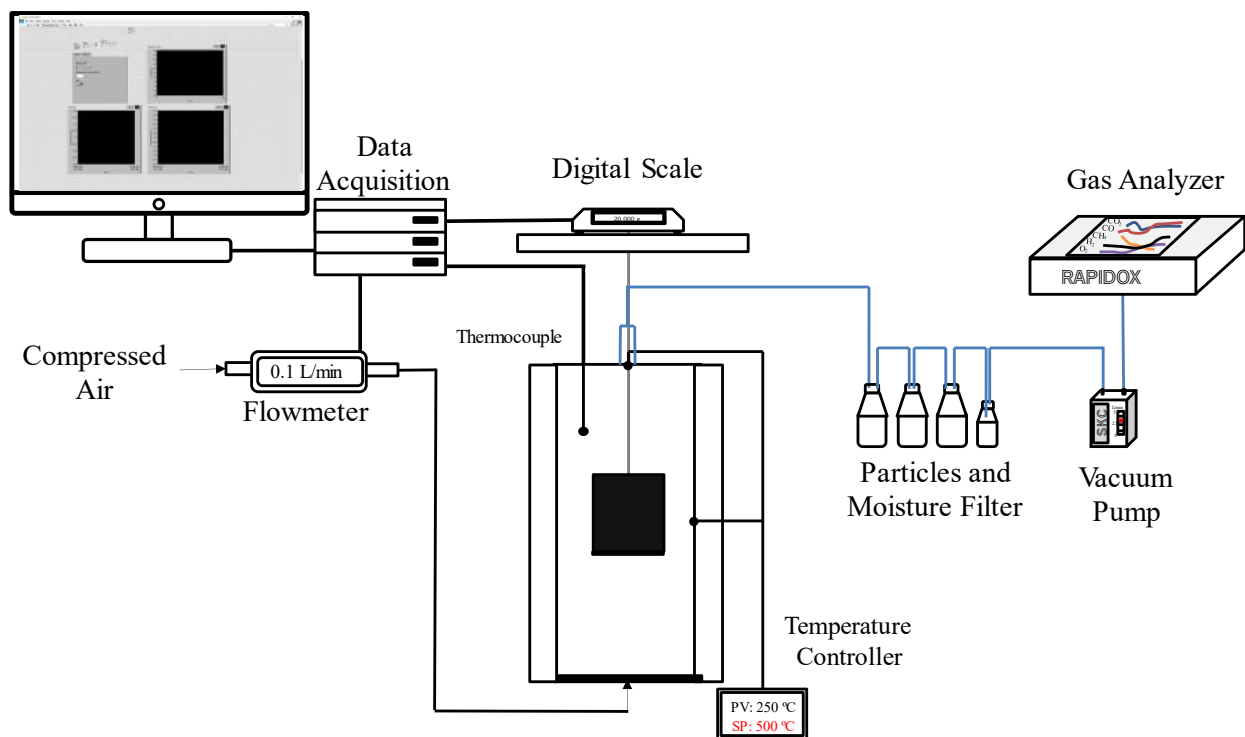
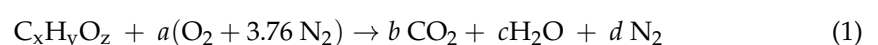


Figure 1. Experimental apparatus.

Regarding the experimental procedure, the small-scale reactor was turned on and preheated to the desired temperature before each experiment. The temperatures considered in this work were 400 and 800 °C in order to present a comprehensive view of biomass conversion over a wide temperature range. Inside the reactor, the walls radiated heat to the surface of the basket, which was in the middle of the reactor. The perforated basket allowed for an air flow to enter and react with the woodchip particles. After reaching a constant temperature in the reactor, the basket was removed, the sample with approximately 20 g was quickly loaded, and the basket was then introduced back into the reactor.

During each experiment, the air flow was controlled at different air flow rates in order to reproduce gasification and combustion regimes at any desired temperature. The air flow necessary for each conversion regime was determined by using Equations (1) and (2), which represent a stoichiometric combustion reaction and the air-to-fuel ratio ( $\lambda$ ).



$$\lambda = \frac{\frac{m_{air,real}}{m_{fuel}}}{\frac{a \cdot M_{air}}{x \cdot C + y \cdot H + z \cdot O}} \quad (2)$$

Hence, taking into account the elemental composition of the eucalyptus woodchips presented in Table 1 and the reference value of the air-to-fuel ratio for gasification (0.1 to 0.3) and combustion (1.4), the air flow rate used for gasification experiments was 0.1 L/min, 15.5 for combustion experiments, and 50 L/min for experiments using 400 and 800 °C, respectively. The different air flow rates used for experiments at the highest temperature were necessary because the reaction is considerably faster than at 400 °C. The experiments were run in duplicate for 15 and 10 min for experiments at 400 and 800 °C, respectively. The average values were computed and are reported in the following section. The standard deviation during all experiments was not higher than 0.09%.

### 3. Results and Discussion

#### 3.1. Thermochemical Conversion: Mass Loss

The mass loss of the samples of eucalyptus woodchips for gasification and combustion regime is presented in Figure 2. Two distinct zones can be identified, each one with a nearly linear variation with time.

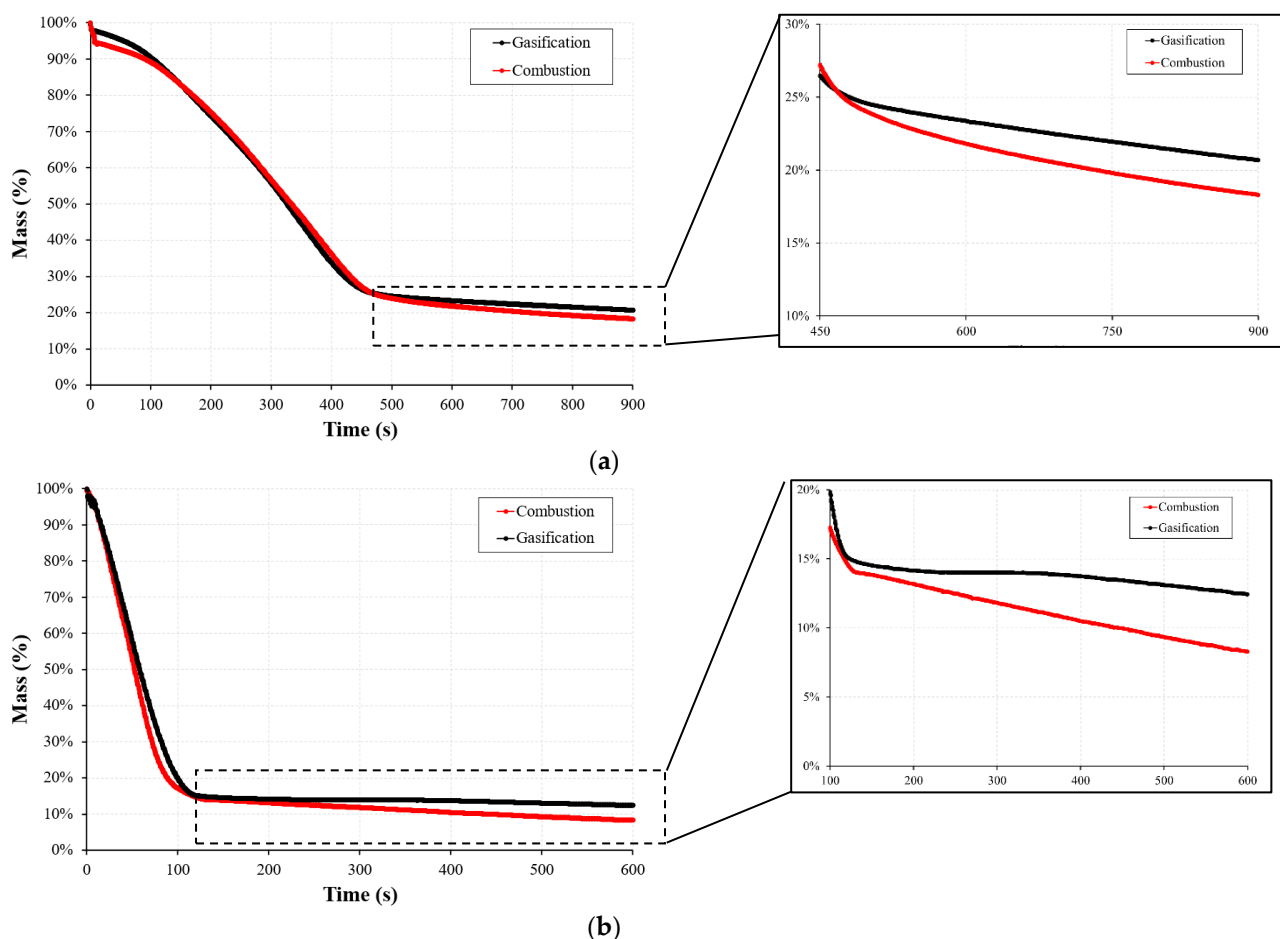


**Figure 2.** Mass loss curves considering the gasification and combustion regime at: (a) 400 °C and (b) 800 °C.

In the first region, which includes both the drying and devolatilization stages, there is no significant difference between gasification and combustion conversion regimes. At 400 °C the average mass loss was 75%, while at 800 °C the mass loss was approximately



85%. This suggests that temperature has a small impact on the sample's mass loss. However, temperature has a major impact on the devolatilization rate. The average mass loss rate detected was 0.16 and 0.72%/s in gasification conditions at 400 and 800 °C, respectively. However, in combustion conditions, the devolatilization rate increases from 0.16 to 0.70%/s at 400 and 800 °C, respectively. This means there is an increase of nearly four times the devolatilization rate by increasing the process temperature from 400 to 800 °C.

However, after the first region, the mass loss decreases over time but at a much slower rate. Hence, when the moisture and volatile matter are completely released, char oxidation starts and the mass loss starts to decrease more slowly. Mau et al. [45] showed this phenomena in his work by performing TGA on several char samples.

Hence, in the second region, it is possible to observe that there are differences between the mass loss curves at different thermochemical conditions and at both temperatures. For this stage, the average mass loss rate was 0.016 and 0.006%/s in gasification conditions at 400 and 800 °C, and 0.024 and 0.012%/s in combustion conditions at 400 and 800 °C, respectively. There are two main characteristics that can be noticed. In the first one, the mass loss rate was higher in combustion conditions, indicating that the presence of air enhances thermal loss due to the higher diffusion of oxygen into the solid biomass particles when compared with reduced oxygen in gasification. Simultaneously, at 400 °C the mass loss rate was higher compared with the tests performed at 800 °C for both conditions. This suggests that the remaining volatile matter that could not be devolatilized in the first stage is used to improve the char oxidation. This is in agreement to the review by Li [46] in which the author demonstrated the importance of the volatile-char interactions during the gasification process.

Furthermore, another important issue that can be observed by analyzing the mass loss curves is that the drying and devolatilization stages happen at the same time. One of the reasons might be because the moisture content of the samples was not so significant. However, higher moisture content can introduce some variance on the mass loss on a TGA experiment [47]. As it can be observed, there are no variations of the mass loss in the early stages, which states clearly that the gasification and combustion processes of larger particles do not have the sequence of distinct conversion stages when large particles are burned. In smaller samples, these two steps can be clearly identified as separate events, as the thermal gradients inside the particles are negligible [48]. Table 2 presents some characteristic parameters of the mass loss curves, which corroborate the abovementioned findings. Additionally, the results of the final mass suggest that char conversion also depends on the environment temperature. This fact is highlighted by the difference observed in the result between the experiments at low and high temperatures. Hence, mass transfer (diffusion of oxygen) and kinetics control the second mass region.

**Table 2.** Characteristic parameters of the mass loss curves at different regimes of thermochemical conversion in the same period of the experiment (600 s).

Temperature	Mass Loss—1st Stage (%)	Devolatilization Time (s)	Final Mass (%)
Gasification			
400 °C	74.49	466	23.35
800 °C	84.60	117	12.44
Combustion			
400 °C	75.19	477	21.80
800 °C	85.80	126	8.30

### 3.2. Gas Release: Product Distribution

The gases released during all conversion periods were collected. Figure 3 presents the average results from these experiments and shows, in particular, that gaseous emissions are strongly dependent on the operating temperature and the thermochemical conversion

regime. The standard deviation during all experiments was not higher than 0.5%. The remaining volume percentage corresponds to the nitrogen and oxygen content.

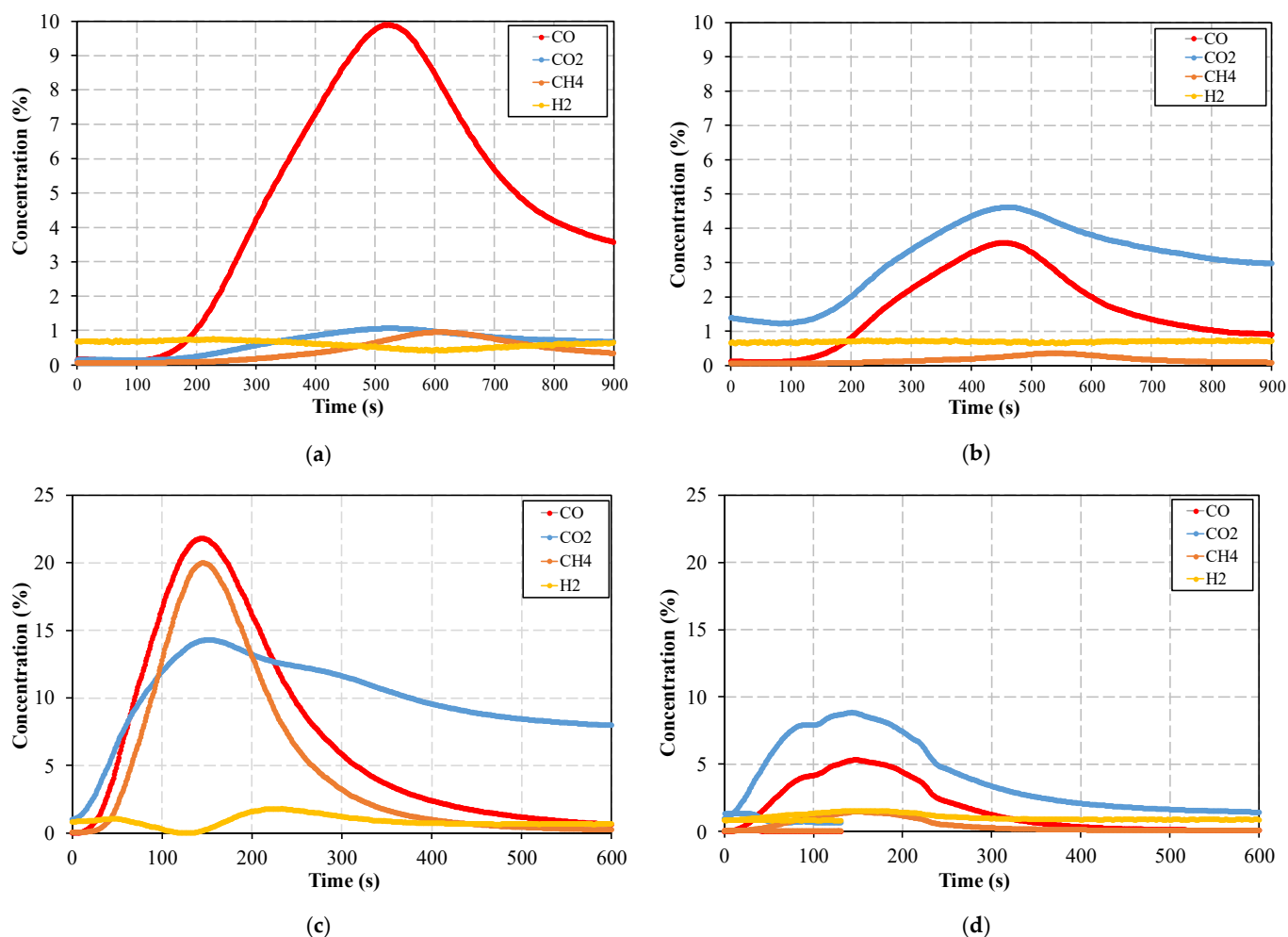


**Figure 3.** Gas emissions at different reactor temperatures and conversion conditions: (a) gasification at 400 °C, (b) combustion at 400 °C, (c) gasification at 800 °C, (d) combustion at 800 °C.

A similar trend was reported by Neves et al. [42], where it was found that at temperatures above 500 °C, the gaseous products strongly become temperature-dependent, leading to a substantial increase in the CO mass fractions. This was considered a result of secondary reactions, which resulted in the decrease in the tar mass fraction, also due to the conversion to CH<sub>4</sub>. The same behavior was described by Mehrabian et al. [43] based on dedicated experiments and data collected from the literature. Secondary reactions of the volatiles are negligible at low temperatures, and most of the permanent gases result directly from biomass thermal degradation. Within the low temperature range, gases like CO and CO<sub>2</sub> are the main permanent gas compounds with low quantities of CH<sub>4</sub>. As the temperature increases, secondary reactions occur, and an increase in CO and CH<sub>4</sub> are attributed to the decrease of tar. Here, due to higher temperatures, the yields of the volatiles have a strong correlation with the temperature and CO is considered responsible for the conversion of two-thirds of the tar.

Although the tar was not measured during the experiments, the results are in accordance with the theory. As depicted in Figure 3, there is a considerable increment of the CO from 10 to 21%, CH<sub>4</sub> from 1 to 20%, and CO<sub>2</sub> from 1 to almost 15% (peak) in gasification conditions, when increasing the temperature. In combustion conditions, the increase in temperature also enhanced the concentration of CO and CO<sub>2</sub> from 3.5 to 5% and 4.5 to 9%, respectively. Regarding the influence of the air in the process, at 400 °C, increasing the air



flow rate enhanced the combustion process by converting the CO into CO<sub>2</sub>. At 800 °C, once again, the air revealed a major influence on gas conversion, specifically for the CO and CH<sub>4</sub> that decreased their concentration from 21 to 5% and 20 to 1%, respectively. This fact is in line with the previously mentioned findings reported in the literature. To quantify the differences between both conversion regimes and the influence of the reactor temperature, the volume of each gas compound, as well as their average value, was computed during the experiment. Table 3 presents these values and it is possible to observe that all gas compounds, except H<sub>2</sub>, increased when the experiment was developed at 800 °C, particularly in sub-stoichiometric conditions.

**Table 3.** Normalized gas emissions considering the different regimes of thermochemical conversion, temperatures, and the duration of the experiment (600 s). The numbers in brackets refer to the average percentage during the experiment.

Value (L/g Biomass)	Gasification		Combustion	
	400 °C	800 °C	400 °C	800 °C
CO <sub>2</sub>	0.32 (0.57)	3.96 (9.99)	1.43 (3.01)	1.28 (4.05)
CO	2.58 (4.50)	2.79 (7.07)	0.86 (1.82)	0.53 (1.73)
CH <sub>4</sub>	0.18 (0.30)	2.02 (5.13)	0.08 (0.17)	0.13 (0.44)
H <sub>2</sub>	0.32 (0.63)	0.34 (0.87)	0.32 (0.69)	0.36 (1.06)

#### 4. Conclusions

This work presented a purpose-built facility developed to study how solid biomass fuels behave in conditions similar to those found in industrial power plants. This work stands out from the major of macro TGA in literature as it employs a single work temperature in contrast to the usual increase of the temperature on a fixed heating rate [38,49]. From a practical point of view, this information may be valuable for developing mathematical models. Hence, the mass loss profiles at different thermochemical conditions of eucalyptus woodchips are presented together with the composition of the gases released over time at two different temperatures.

The reactor proved to be a very useful equipment to analyze the combustion behavior, study the phenomena, which are relevant in an industrial furnace on a small scale, and demonstrated good reproducibility. Furthermore, the weight loss and the release quantification of the different gas compounds were particularly important to expose the differences between the different thermochemical conversion regimes. The main results and findings led to the following conclusions:

- Mainly due to the low moisture content, only two different stages can characterize the mass loss of eucalyptus woodchips at low and high temperatures with different kinetics for both thermochemical regimes.
- The first region, which corresponds to a mass loss of 75 to 85% (gasification and combustion, respectively), does not present the influence of the air flow rate, which defines the thermochemical conversion condition; however, there is a significant difference between gasification and combustion conversion at different temperatures. Therefore, the kinetics of the reaction in the devolatilization stage is mainly dependent on the temperature.
- The second conversion stage, in its turn, is dependent on the air flow rate and, therefore, dependent on the diffusion of the oxygen supplied to the solid biomass particles. However, it was verified that at the lowest reactor temperature this reaction presented a contribution of the temperature. This might be related to the remaining volatile matter that was not consumed in the devolatilization stage and was used to react with the remaining carbon.
- Regarding the gases released during all conversion periods, a strong dependency on the reactor temperature and the thermochemical conversion regime was observed.

- All gas compounds, except H<sub>2</sub>, increased substantially with reactor temperature and, mainly, when gasification occurred. This suggests that the success of obtaining a better combustible gas during the gasification process depends substantially on process temperature [50].
- The yield of the lowest temperature, comparing both thermochemical conversion conditions, the CO and CO<sub>2</sub> emissions are approximately 3 times higher when gasification occurs. However, at 800 °C, the same trend was verified, while a considerable amount of CH<sub>4</sub> was also verified.
- The gas emissions also showed the impact of the air injection in the conversion of combustible gases and in non-combustible gases. By increasing the CO<sub>2</sub>, CO, and CH<sub>4</sub>, concentrations for both temperatures were reduced.
- The measurement of the gas emissions in the purpose-built facility also demonstrated a useful strategy to further define the correct boundary conditions for CFD simulations.

For future work, data concerning reaction kinetics and gas emissions will be incorporated into a numerical model to describe the thermochemical conversion behavior inside an industrial grate-fired boiler. This type of information is one of the main drawbacks of commercial simulation software. Additionally, this approach extends to other types of fuels whose behavior is less understood.

**Author Contributions:** Conceptualization, J.S., C.C. and J.T.; Methodology, J.S., C.C. and J.T.; Investigation, J.S.; Writing—original draft preparation, J.S., C.C., J.T. and S.T.; Writing—review and editing, J.S., C.C., J.T. and S.T.; Supervision, J.T. and S.T. All authors have read and agreed to the published version of the manuscript.

**Funding:** This work was supported by the Portuguese Foundation for Science and Technology (FCT) within the R&D Units Project Scope UIDB/00319/2020 (ALGORITMI), and R&D Units Project Scope UIDP/04077/2020 (METRICS).

**Institutional Review Board Statement:** Not applicable.

**Informed Consent Statement:** Not applicable.

**Acknowledgments:** The first author would like to express his gratitude for the support given by FCT through the Ph.D. Grant SFRH/BD/130588/2017.

**Conflicts of Interest:** The authors declare no conflict of interest.

## References

1. Demirbas, A. Potential applications of renewable energy sources, biomass combustion problems in boiler power systems and combustion related environmental issues. *Prog. Energy Combust. Sci.* **2005**, *31*, 171–192. [CrossRef]
2. Ferreira, S.; Monteiro, E.; Brito, P.; Vilarinho, C. Biomass resources in Portugal: Current status and prospects. *Renew. Sustain. Energy Rev.* **2017**, *78*, 1221–1235. [CrossRef]
3. GPP—Gabinete de Planeamento Políticas e Administração Geral. Caderno de Análise e Prospetiva Cultivar. 2018. Available online: <https://doi.org/2183-5624> (accessed on 11 September 2022).
4. Roman, K.; Barwicki, J.; Rządowicz, W.; Dawidowski, M. Evaluation of Mechanical and Energetic Properties of the Forest Residues Shredded Chips during Briquetting Process. *Energies* **2021**, *14*, 3270. [CrossRef]
5. Anca-Couce, A.; Hochenauer, C.; Scharler, R. Bioenergy technologies, uses, market and future trends with Austria as a case study. *Renew. Sustain. Energy Rev.* **2020**, *135*, 110237. [CrossRef]
6. Basu, P. *Biomass Gasification, Pyrolysis and Torrefaction: Practical Design and Theory*, 2nd ed.; Elsevier Inc.: Amsterdam, The Netherlands, 2013; p. 530. [CrossRef]
7. Vainio, E. Fate of Fuel-Bound Nitrogen and Sulfur in Biomass-Fired Industrial Boilers. Ph.D. Thesis, Åbo Akademi University, Turku, Finland, 2014.
8. Sadaka, S.; Johnson, D. Biomass Combustion. Agriculture and Natural Resources. 2010. Available online: [https://www.researchgate.net/publication/268207461\\_Biomass\\_Combustion](https://www.researchgate.net/publication/268207461_Biomass_Combustion) (accessed on 11 September 2022).
9. Kirch, T.; Birzer, C.; van Eyk, P.; Medwell, P.R. Influence of Primary and Secondary Air Supply on Gaseous Emissions from a Small-Scale Staged Solid Biomass Fuel Combustor. *Energy Fuels* **2017**, *32*, 4212–4220. [CrossRef]
10. Sun, J.; Shen, Z.; Zhang, L.; Zhang, Q.; Lei, Y.; Cao, J.; Huang, Y.; Liu, S.; Zheng, C.; Xu, H.; et al. Impact of primary and secondary air supply intensity in stove on emissions of size-segregated particulate matter and carbonaceous aerosols from apple tree wood burning. *Atmos. Res.* **2017**, *202*, 33–39. [CrossRef]

11. Yin, C.; Rosendahl, L.A.; Kær, S.K. Grate-firing of biomass for heat and power production. *Prog. Energy Combust. Sci.* **2008**, *34*, 725–754. [[CrossRef](#)]
12. Perera, S.M.; Wickramasinghe, C.; Samarasiri, B.; Narayana, M. Modeling of thermochemical conversion of waste biomass—A comprehensive review. *Biofuel Res. J.* **2021**, *8*, 1481–1528. [[CrossRef](#)]
13. Ragland, K.; Aerts, D.; Baker, A. Properties of wood for combustion analysis. *Bioresour. Technol.* **1991**, *37*, 161–168. [[CrossRef](#)]
14. Hellén, H.; Hakola, H.; Haaparanta, S.; Pietarila, H.; Kauhaniemi, M. Influence of residential wood combustion on local air quality. *Sci. Total Environ.* **2008**, *393*, 283–290. [[CrossRef](#)]
15. Jia, Y.; Li, Z.; Wang, Y.; Wang, X.; Lou, C.; Xiao, B.; Lim, M. Visualization of Combustion Phases of Biomass Particles: Effects of Fuel Properties. *ACS Omega* **2021**, *6*, 27702–27710. [[CrossRef](#)] [[PubMed](#)]
16. Grønli, M.G.; Varhegyi, G.; Di Blasi, C. Thermogravimetric Analysis and Devolatilization Kinetics of Wood. *Ind. Eng. Chem. Res.* **2002**, *41*, 4201–4208. [[CrossRef](#)]
17. Chen, Z.; Hu, M.; Zhu, X.; Guo, D.; Liu, S.; Hu, Z.; Xiao, B.; Wang, J.; Laghari, M. Characteristics and kinetic study on pyrolysis of five lignocellulosic biomass via thermogravimetric analysis. *Bioresour. Technol.* **2015**, *192*, 441–450. [[CrossRef](#)]
18. Mishra, R.K.; Mohanty, K. Pyrolysis kinetics and thermal behavior of waste sawdust biomass using thermogravimetric analysis. *Bioresour. Technol.* **2018**, *251*, 63–74. [[CrossRef](#)] [[PubMed](#)]
19. Xiao, R.; Yang, W.; Cong, X.; Dong, K.; Xu, J.; Wang, D.; Yang, X. Thermogravimetric analysis and reaction kinetics of lignocellulosic biomass pyrolysis. *Energy* **2020**, *201*, 117537. [[CrossRef](#)]
20. Gaitán-Álvarez, J.; Moya, R.; Puente-Urbina, A.; Rodríguez-Zuñiga, A. Thermogravimetric, Devolatilization Rate, and Differential Scanning Calorimetry Analyses of Biomass of Tropical Plantation Species of Costa Rica Torrefied at Different Temperatures and Times. *Energies* **2018**, *11*, 696. [[CrossRef](#)]
21. Fernandez, A.; Soria, J.; Rodriguez, R.; Baeyens, J.; Mazza, G. Macro-TGA steam-assisted gasification of lignocellulosic wastes. *J. Environ. Manag.* **2018**, *233*, 626–635. [[CrossRef](#)]
22. Becidan, M.; Skreiberg, Ø.; Hustad, J.E. Products distribution and gas release in pyrolysis of thermally thick biomass residues samples. *J. Anal. Appl. Pyrolysis* **2007**, *78*, 207–213. [[CrossRef](#)]
23. Brunner, T.; Biedermann, F.; Kanzian, W.; Evic, N.; Obernberger, I. Advanced Biomass Fuel Characterization Based on Tests with a Specially Designed Lab-Scale Reactor. *Energy Fuels* **2013**, *27*, 5691–5698. [[CrossRef](#)]
24. Gauthier, G.; Melkior, T.; Grateau, M.; Thiery, S.; Salvador, S. Pyrolysis of centimetre-scale wood particles: New experimental developments and results. *J. Anal. Appl. Pyrolysis* **2013**, *104*, 521–530. [[CrossRef](#)]
25. Weissinger, A. In situ FT-IR spectroscopic investigations of species from biomass fuels in a laboratory-scale combustor: The release of nitrogenous species. *Combust. Flame* **2004**, *137*, 403–417. [[CrossRef](#)]
26. Bennadji, H.; Smith, K.; Shabangu, S.; Fisher, E. Low-Temperature Pyrolysis of Woody Biomass in the Thermally Thick Regime. *Energy Fuels* **2013**, *27*, 1453–1459. [[CrossRef](#)]
27. Nikku, M.; Deb, A.; Sermyagina, E.; Puro, L. Reactivity characterization of municipal solid waste and biomass. *Fuel* **2019**, *254*, 115690. [[CrossRef](#)]
28. Hu, Q.; He, X.; Yao, Z.; Dai, Y.; Wang, C.-H. Gaseous production kinetics and solid structure analysis during isothermal conversion of biomass pellet under different atmospheres. *J. Energy Inst.* **2021**, *98*, 53–62. [[CrossRef](#)]
29. Baumgarten, B.; Reinhardt, J.; Lepski, C.; Risio, B.; Thorwarth, H. Kinetics of Wood Devolatilization during Start-up. *Energy Fuels* **2019**, *33*, 11285–11291. [[CrossRef](#)]
30. Samuelsson, L.N.; Umeki, K.; Babler, M.U. Mass loss rates for wood chips at isothermal pyrolysis conditions: A comparison with low heating rate powder data. *Fuel Process. Technol.* **2017**, *158*, 26–34. [[CrossRef](#)]
31. Orang, N.; Tran, H. Effect of feedstock moisture content on biomass boiler operation. *TAPPI J.* **2015**, *14*, 629–637. [[CrossRef](#)]
32. Bin Yang, Y.; Ryu, C.; Khor, A.; Sharifi, V.N.; Swithenbank, J. Fuel size effect on pinewood combustion in a packed bed. *Fuel* **2005**, *84*, 2026–2038. [[CrossRef](#)]
33. Ryu, C.; Yang, Y.B.; Khor, A.; Yates, N.E.; Sharifi, V.N.; Swithenbank, J. Effect of fuel properties on biomass combustion: Part I. Experiments—Fuel type, equivalence ratio and particle size. *Fuel* **2006**, *85*, 1039–1046. [[CrossRef](#)]
34. Mahmoudi, A.H.; Markovic, M.; Peters, B.; Brem, G. An experimental and numerical study of wood combustion in a fixed bed using Euler–Lagrange approach (XDEM). *Fuel* **2015**, *150*, 573–582. [[CrossRef](#)]
35. Wurzenberger, J.C.; Wallner, S.; Raupenstrauch, H.; Khinast, J. Thermal conversion of biomass: Comprehensive reactor and particle modeling. *AIChE J.* **2002**, *48*, 2398–2411. [[CrossRef](#)]
36. Markovic, M.; Bramer, E.A.; Brem, G. Experimental investigation of wood combustion in a fixed bed with hot air. *Waste Manag.* **2014**, *34*, 49–62. [[CrossRef](#)] [[PubMed](#)]
37. Erić, A.; Nemoda, S.; Komatina, M.; Dakić, D.; Repić, B. Experimental investigation on the kinetics of biomass combustion in vertical tube reactor. *J. Energy Inst.* **2019**, *92*, 1077–1090. [[CrossRef](#)]
38. Long, Y.; Zhou, H.; Meng, A.; Li, Q.; Zhang, Y. Interactions among biomass components during co-pyrolysis in (macro)thermogravimetric analyzers. *Korean J. Chem. Eng.* **2016**, *33*, 2638–2643. [[CrossRef](#)]
39. Fraga, L.G.; Silva, J.; Teixeira, J.C.; Ferreira, M.E.C.; Teixeira, S.F.; Vilarinho, C.; Gonçalves, M.M. Study of Mass Loss and Elemental Analysis of Pine Wood Pellets in a Small-Scale Reactor. *Energies* **2022**, *15*, 5253. [[CrossRef](#)]
40. Jiang, M.; Lai, A.; Law, A. Solid Waste Incineration Modelling for Advanced Moving Grate Incinerators. *Sustainability* **2020**, *12*, 8007. [[CrossRef](#)]

41. Thunman, H.; Niklasson, F.; Johnsson, F.; Leckner, B. Composition of Volatile Gases and Thermochemical Properties of Wood for Modeling of Fixed or Fluidized Beds. *Energy Fuels* **2001**, *15*, 1488–1497. [[CrossRef](#)]
42. Neves, D.; Thunman, H.; Matos, A.; Tarelho, L.; Gómez-Barea, A. Characterization and prediction of biomass pyrolysis products. *Prog. Energy Combust. Sci.* **2011**, *37*, 611–630. [[CrossRef](#)]
43. Mehrabian, R.; Shiehnejadhesar, A.; Scharler, R.; Obernberger, I. Multi-physics modelling of packed bed biomass combustion. *Fuel* **2014**, *122*, 164–178. [[CrossRef](#)]
44. Silva, J.P.; Teixeira, S.; Grilo, É.; Peters, B.; Teixeira, J.C. Analysis and monitoring of the combustion performance in a biomass power plant. *Clean. Eng. Technol.* **2021**, *5*, 100334. [[CrossRef](#)]
45. Mau, V.; Gross, A. Energy conversion and gas emissions from production and combustion of poultry-litter-derived hydrochar and biochar. *Appl. Energy* **2018**, *213*, 510–519. [[CrossRef](#)]
46. Li, C.-Z. Importance of volatile–char interactions during the pyrolysis and gasification of low-rank fuels—A review. *Fuel* **2013**, *112*, 609–623. [[CrossRef](#)]
47. Magdziarz, A.; Werle, S. Analysis of the combustion and pyrolysis of dried sewage sludge by TGA and MS. *Waste Manag.* **2014**, *34*, 174–179. [[CrossRef](#)]
48. Fraga, L.G.; Silva, J.; Teixeira, S.; Soares, D.; Ferreira, M.; Teixeira, J. Influence of Operating Conditions on the Thermal Behavior and Kinetics of Pine Wood Particles Using Thermogravimetric Analysis. *Energies* **2020**, *13*, 2756. [[CrossRef](#)]
49. Skreiberg, A.; Sandquist, J.; Sørum, L. TGA and macro-TGA characterisation of biomass fuels and fuel mixtures. *Fuel* **2011**, *90*, 2182–2197. [[CrossRef](#)]
50. Basu, P. *Biomass Gasification, Pyrolysis and Torrefaction: Practical Design and Theory*, 3rd ed.; Academic Press: Cambridge, MA, USA, 2018. [[CrossRef](#)]